Many-Body Effects on High-Harmonic Generation in Hubbard Ladders

Yuta Murakami,[1,2] Thomas Hansen,[3] Shintaro Takayoshi,[4] Lars Bojer Madsen,[3] and Philipp Werner[5]
[1]Institute for Materials Research, Tohoku University, Sendai 980-8577, Japan
[2]Center for Emergent Matter Science, RIKEN, Wako, Saitama 351-0198, Japan
[3]Department of Physics and Astronomy, Aarhus University, Ny Munkegade 120, DK-8000 Aarhus C, Denmark
[4]Department of Physics, Konan University, Kobe 658-8501, Japan
[5]Department of Physics, University of Fribourg, 1700 Fribourg, Switzerland

(Received 2 July 2024; accepted 7 February 2025; published 7 March 2025)

We unveil multifaceted effects of spin-charge couplings on the high-harmonic generation (HHG) in Mott insulators by analyzing the two-leg ladder Hubbard model, where spin dynamics activated by the interchain hopping t_y drastically modifies the HHG features. When the two chains are decoupled ($t_y = 0$), HHG originates from the dynamics of coherent doublon-holon pairs because of spin-charge separation. With increasing t_y, the doublon-holon pairs lose their coherence due to their interchain hopping and resultant nonlocal spin strings. Furthermore, the HHG signal from spin polarons—charges dressed by spin clouds—leads to an additional plateau in the HHG spectrum. For large t_y, we identify unconventional HHG processes involving *three* elementary excitations—two polarons and one magnon. Our study is an essential step toward a microscopic understanding of nontrivial many-body effects on HHG in correlated materials beyond conventional semiconductors.

DOI: 10.1103/PhysRevLett.134.096504

Introduction—High-harmonic generation (HHG) is a fundamental and technologically important optical phenomenon originating from strong light-matter interaction [1–4]. In the past decade, HHG research expanded from gases [5–7] to solids [8–11], opening up new possibilities for optical and spectroscopic applications [12]. To date, most HHG research in solids focuses on semiconductors and semimetals [8,13–34], where HHG is well described by the kinematics of independent electrons. Recently, the investigations were further extended to correlated materials, where the independent-electron picture does not directly apply [35–38]. Although previous studies revealed some intriguing effects, such as HHG from many-body states [36,39] and changes in the charge trajectory during the HHG process [38], the broader implications of correlations on HHG remain to be clarified.

Strongly correlated systems (SCSs) provide a rich playground for studying many-body effects on HHG [35–37,39–66]. In SCSs, various degrees of freedom such as charge, spin, and orbital are intertwined and the conventional band picture is not applicable [67–69]. Instead, the system can host intriguing excitation structures, which can lead to nontrivial HHG features. Theoretically, SCSs are often represented by the Hubbard model, where strong local interactions lead to a Mott insulating state at half-filling. Previous works revealed that HHG in Mott insulators can be associated with the coherent dynamics of charged many-body elementary excitations called doublons (doubly occupied sites) and holons (empty sites) [36,44]. To fully understand the charge dynamics in Mott insulators, it is however crucial to consider spin-charge couplings, i.e., the modification of the spin background by the charge motion. This physics becomes relevant in generic systems, beyond the previously studied one-dimensional chains [35,44,50]. Indeed, such couplings can lead to an intriguing temperature dependence of HHG [51,52]. However, only limited aspects of the spin-charge couplings have been explored so far and a generic understanding of their impact on HHG remains elusive. In particular, potentially relevant effects, such as the formation of spin strings and the emergence of new elementary excitations [70,71], have not been discussed.

Through a comprehensive analysis of the two-leg Hubbard model, we reveal that the effects of the intertwined spin-charge dynamics on HHG in Mott insulators are multifaceted. This is because spin-charge couplings affect the nature of elementary excitations in unique and complex manners. Because of its geometric structure, the two-leg system is a natural step beyond the one-dimensional chain, allowing us to discuss the physics of spin-charge couplings. The many-body effects revealed here may be relevant for generic two-dimensional systems, and will contribute to the broader understanding of HHG in SCSs.

Formulation—We focus on the half-filled Hubbard model defined on the two-leg ladder [72,73]

$$\hat{H}(t) = -t_x \sum_{i_x,i_y,\sigma} (e^{iA_x(t)} \hat{c}^\dagger_{i_x+1 i_y \sigma} \hat{c}_{i_x i_y \sigma} + \text{H.c.}) - t_y \sum_{i_x,\sigma} (\hat{c}^\dagger_{i_x 0 \sigma} \hat{c}_{i_x 1 \sigma} + \text{H.c.}) + \hat{H}_U, \quad (1)$$

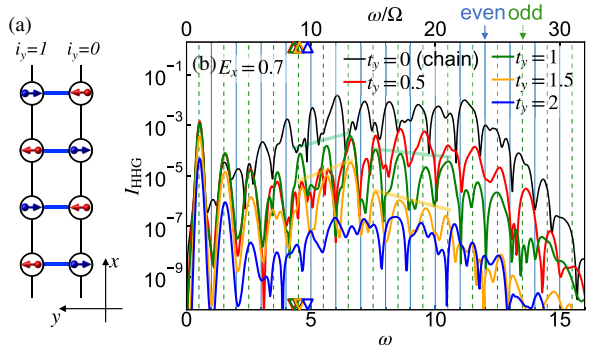

FIG. 1. (a) Schematic picture of the half-filled two-leg Hubbard model. (b) HHG spectra for the half-filled two-leg Hubbard model for different t_y, see Eq. (1). We use $t_x = 1$ and $U = 8$, and set $\Omega = 0.5$, $E_x = 0.7$, $t_0 = 60$, and $\sigma_0 = 15$ for the electric field. The triangle markers indicate the optical gaps for each t_y, and the green (orange) transparent lines indicate the two plateaulike structures for $t_y = 1$ (1.5).

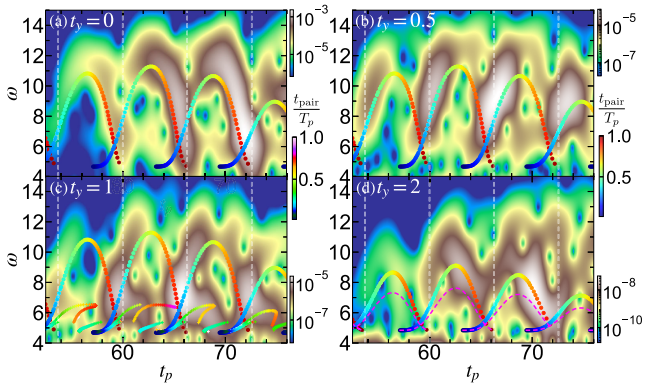

FIG. 2. Subcycle spectra for the data in Fig. 1(b) shown on a log scale, based on a Gaussian window with $\sigma_p = 0.8$. The vertical dashed lines indicate the times with $A_x(t) = 0$. The multicolored markers and the pink dashed lines indicate the energy emission at time t_p within the three-step model. In (a)–(c), the dots (•) are for the DH pairs, whose dispersion is obtained from the chain system. In (c), the crosses (+) are for the spin-polaron pairs, whose dispersion is obtained from Fig. 4(b). In (d), the dots are for scenario 1 (hPolaron + ePolaron + magnon), while the pink dashed line is for scenario 2 (hPolaron + spin bag). The color bars cover the time interval between creation and recombination of the corresponding pair in units of $T_p = (2\pi/\Omega)$.

see Fig. 1(a). Here $\hat{c}^{\dagger}_{i_x i_y \sigma}$ is the creation operator for an electron with spin σ, i_x (i_y) is the site index in the x (y) direction, and $\hat{n}_{i_x i_y \sigma} = \hat{c}^{\dagger}_{i_x i_y \sigma}\hat{c}_{i_x i_y \sigma}$. t_x and t_y are the hopping parameters and $\hat{H}_U \equiv U\sum_{i_x,i_y}\hat{n}_{i_x i_y \uparrow}\hat{n}_{i_x i_y \downarrow}$ represents the on-site Coulomb interaction. The electric field is applied along x, and its effect is described by the Peierls phase with the vector potential $A_x(t)$. The corresponding electric field is $E_x(t) = -\partial_t A_x(t)$, and we use a Gaussian pulse $A_x(t) = (E_x/\Omega) F_G(t-t_0,\sigma_0)\sin[\Omega(t-t_0)]$ with $F_G(t,\sigma) = \exp\{-[t^2/(2\sigma^2)]\}$. We set the electronic charge q, the bond length, and $\hbar$ to unity. In the following, we use t_x as the unit of energy and choose $U = 8$, where the system is in the Mott insulating phase [74,75]. We use $\Omega = 0.5$, $t_0 = 60$, and $\sigma_0 = 15$ for the pump. This parameter set is motivated by two-leg cuprates such as $SrCu_2O_3$ [76,77] excited by a midinfrared laser, for which our energy unit roughly corresponds to 0.5 eV. We analyze the dynamics from the ground state using the infinite time-evolving block decimation (iTEBD), which treats the thermodynamic limit and is highly controllable [78]. The HHG spectrum is evaluated as $I_{\mathrm{HHG}}(\omega) = |\omega J_x(\omega)|^2$, where $J_x(\omega)$ is the Fourier component of the current $J_x(t)$ along x, see Supplemental Material (SM) for details [79]. Because of the inversion symmetry, odd-harmonic peaks at $\omega = (2n+1)\Omega$ with $n \in \mathbb{N}$ are expected in fully time-periodic states [94].

Results—We first show that the qualitative features of HHG drastically change as a function of t_y, see Fig. 1(b) for $E_x = 0.7$. For $t_y = 0$ (two decoupled chains), peak structures at $\omega = (2n+1)\Omega$ are not clear and signals at non-odd-integer harmonics appear, see also SM for different E_x. With increasing t_y, the HHG peaks become more prominent in general and develop around $(2n+1)\Omega$ (dashed lines), as expected, see $t_y = 0.5$, 1, and 1.5. Additionally, signals just above the gap evolve nonmonotonically as a function of t_y. For $t_y = 1$ (relevant for cuprates [77]) and $t_y = 1.5$, a new hump structure around $\omega = 6.5$ develops, which results in two plateaulike structures above the gap ($4.5 \lesssim \omega \lesssim 6.5$ and $6.5 \lesssim \omega \lesssim 10.5$). The hump position increases with increasing field strength (see SM), indicating that this feature does not originate from a specific excitation mode. When the interchain hopping t_y is increased further, HHG peaks become less pronounced and non-odd-integer harmonics appear, as for $t_y = 0$.

To understand the origin of the above changes in HHG, we conduct a subcycle analysis. Specifically, we apply the windowed Fourier transform $J_x(\omega,t_p) = \int dt e^{i\omega t} F_G(t-t_p,\sigma_p) J_x(t)$ and extract the temporal radiation spectrum around t_p as $I(\omega,t_p) = |\omega J_x(\omega,t_p)|^2$. The results are shown in Fig. 2, where the rainbow-colored dots in Figs. 2(a)–2(c) represent the prediction from the semiclassical three-step model for the DH pair [44], see SM. Here, the doublon-holon (DH) dispersion for the chain ($t_y = 0$) is used. The dot color indicates the time between the creation and recombination of the corresponding DH pair. For $t_y = 0$, the temporal change of the radiation intensity is well described by the three-step model and the radiation is mainly emitted by long-lived DH pairs, which is attributed to the spin-charge separation [44]. Upon increasing t_y to 0.5, we notice a reduction of the DH coherence, as manifested by the shift of the weight of $I(\omega,t_p)$ to the subcycle interval corresponding to short-lived DH pairs. Thus, the difference of the HHG features between $t_y = 0$ and $t_y = 0.5$ is related to the DH

coherence. The non-odd-integer harmonics for $t_y = 0$ indicate that the system is not yet fully time periodic, due to a relatively short pump pulse and the long coherence time. The latter allows the system to remember the excitation process, preventing it from reaching a time-periodic state [95] and making the HHG spectrum sensitive to the carrier-envelope phase [33]. A reduction of coherence leads to a faster relaxation into a time-periodic state.

At $t_y = 1$, the subcycle signals are fractionalized into the part explained by the trajectory of the (short-lived) DH pair and a low-lying dispersive signal around $4.5 \lesssim \omega \lesssim 6.5$. The latter appears to originate from the field-driven dynamics of elementary excitations different from DH pairs. This fractionalization manifests itself in the emergence of two plateaulike structures in the HHG signal. For $t_y = 2$, the weight of $I(\omega, t_p)$ is shifted back to later in the cycle of the electric field, which suggests the existence of photocarriers with long coherence. This coherence prevents the system from reaching a time-periodic state during the pump pulse.

Since the drastic changes in HHG with interchain hopping are absent in conventional semiconductors (see SM), they are linked to the strongly correlated nature of the system. Below, we demonstrate that these changes manifest different aspects of intertwined spin-charge dynamics.

First, we reveal the intriguing dephasing mechanism of a DH pair. To this end, we analyze an effective model obtained by the Schrieffer-Wolff transformation, i.e., an expansion in $t_{x,y}/U$ [44,96,97]. The Hamiltonian reads

$$\hat{H}_{\mathrm{eff}}(t) = \hat{H}_{\mathrm{DH}}(t) + \hat{H}_{\mathrm{spin}} + \hat{H}_U - E_x(t)\hat{P}_x(t), \quad (2)$$

where

$$\begin{aligned}\hat{H}_{\mathrm{DH}}(t) = &-t_y \sum_{i_x,\sigma} \hat{\bar{n}}_{i_x 0\bar{\sigma}} (\hat{c}^{\dagger}_{i_x 0\sigma} \hat{c}_{i_x 1\sigma} + \mathrm{H.c.}) \hat{\bar{n}}_{i_x 1\bar{\sigma}} \\ &- t_y \sum_{i_x,\sigma} \hat{n}_{i_x 0\bar{\sigma}} (\hat{c}^{\dagger}_{i_x 0\sigma} \hat{c}_{i_x 1\sigma} + \mathrm{H.c.}) \hat{n}_{i_x 1\bar{\sigma}} \\ &- t_x \sum_{i_x,i_y,\sigma} \hat{\bar{n}}_{i_x+1 i_y\bar{\sigma}} (e^{iA_x(t)} \hat{c}^{\dagger}_{i_x+1 i_y\sigma} \hat{c}_{i_x i_y\sigma} + \mathrm{H.c.}) \hat{\bar{n}}_{i_x i_y\bar{\sigma}} \\ &- t_x \sum_{i_x,i_y,\sigma} \hat{n}_{i_x+1 i_y\bar{\sigma}} (e^{iA_x(t)} \hat{c}^{\dagger}_{i_x+1 i_y\sigma} \hat{c}_{i_x i_y\sigma} + \mathrm{H.c.}) \hat{n}_{i_x i_y\bar{\sigma}}\end{aligned}$$

represents the hopping of doublons and holons. $\bar{\sigma}$ indicates the opposite spin of σ and $\hat{\bar{n}} = (1 - \hat{n})$. $\hat{H}_{\mathrm{spin}} = J_{\mathrm{ex},x} \sum_{i_x,i_y} \hat{\mathbf{s}}_{i_x i_y} \cdot \hat{\mathbf{s}}_{i_x+1 i_y} + J_{\mathrm{ex},y} \sum_{i_x} \hat{\mathbf{s}}_{i_x 0} \cdot \hat{\mathbf{s}}_{i_x 1}$ is the spin exchange term with $J_{\mathrm{ex},x} = 4t_x^2/U$ and $J_{\mathrm{ex},y} = 4t_y^2/U$. $\hat{P}_x(t)$ creates or annihilates a DH pair and acts as an interband dipole moment, see SM for details. This model is an extension of the t-J model [67] to a system with both doublons and holons, and allows us to separate different physical processes related to the DH dynamics [44]. We prepare the initial state as the ground state of $\hat{H}_{\mathrm{spin}}$ with antiferromagnetic correlations, and simulate the time evolution turning off different terms in $\hat{H}_{\mathrm{eff}}(t)$ as (1) $t_y, J_{\mathrm{ex},x}, J_{\mathrm{ex},y} \to 0$, (2) $J_{\mathrm{ex},x}, J_{\mathrm{ex},y} \to 0$, (3) $t_y \to 0$, and (4) no modification. The comparison of cases (1)–(4) provides insights into the role of different physical processes. Namely, the difference between (1) and (2) shows the effects of the DH dynamics along y. Such dynamics does not cost any energy related to the spin exchange coupling, but can disturb the original spin configuration. Meanwhile, the difference between (1) and (3) corresponds to the effect of the energetic coupling originating from the spin mismatch between the chains. This coupling suggests the conversion of the kinetic energy of a doublon or holon into spin exchange energy by disturbing the spin background, whose dephasing effect was discussed previously [52].

In Figs. 3(a) and 3(b), we show the resultant subcycle spectrum for cases (1) and (2). The colored line shows the prediction from the three-step model with the DH dispersion $U - 4t_x \cos(k_x)$. In case (1), where only the DH motion along x is considered, the DH pairs exhibit a long coherence time. Importantly, hoppings of charges along y already cause a substantial reduction of pair coherence, as can be seen by the clear shift of the weight to the early part of the cycle in case (2). Although dephasing is also observed in case (3), for the present parameter set, the effect is much more prominent in case (2), see SM.

The unique dephasing seen in case (2) can be attributed to the emergence of nonlocal spin strings (disturbances of the spin configuration from the ground state) [70,71], see

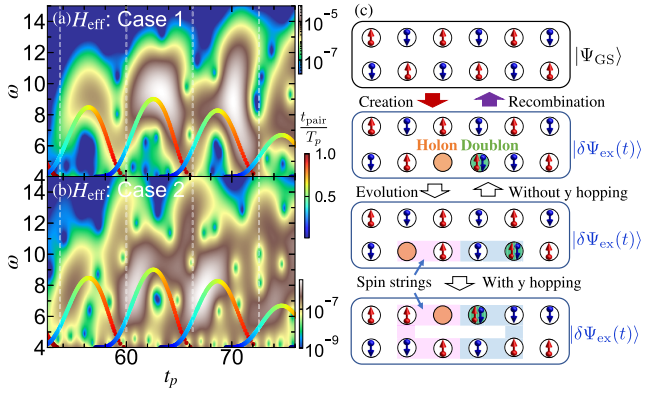

FIG. 3. (a),(b) Subcycle spectra of the two-leg Mott insulator described by the effective model. We use $t_x = 1$, $t_y = 0.5$, $U = 8$ for the system, $\Omega = 0.5$, $E_x = 0.7$, $t_0 = 60$, $\sigma_0 = 15$ for the field pulse, and $\sigma_p = 0.8$ for the analysis. The rainbow-colored dots are the prediction from the three-step model of the DH pair, whose dispersion is $E_g(k_x) = U - 4t_x \cos(k_x)$. (c) Schematic illustration of the effects of DH hopping along y on the light emission. The shaded area indicates the trajectory of the doublon and holon, i.e., the formation of a string in the spin background, which prohibits the return to the ground state by DH recombination.

Fig. 3(c). The HHG spectrum is evaluated from the current $J_x(t) = \langle\Psi(t)|\hat{J}_x|\Psi(t)\rangle$, where $|\Psi(t)\rangle = |\Psi_{\mathrm{GS}}\rangle + |\delta\Psi_{\mathrm{ex}}(t)\rangle$ is the time-dependent wave function, $|\Psi_{\mathrm{GS}}\rangle$ is the Mott insulating ground state, and $|\delta\Psi_{\mathrm{ex}}(t)\rangle$ is an excited state. In the present setup, the deviation from the ground state is small and the major contribution comes from $\langle\Psi_{\mathrm{GS}}|\hat{J}_x|\delta\Psi_{\mathrm{ex}}(t)\rangle$ and its conjugate, which represent the DH recombination. Note that $|\delta\Psi_{\mathrm{ex}}(t)\rangle$ is a superposition of DH pairs with different trajectories. If a trajectory of a DH pair does not involve hopping along y, it contributes to $\langle\Psi_{\mathrm{GS}}|\hat{J}_x|\delta\Psi_{\mathrm{ex}}(t)\rangle$ (recombination) when the pair returns to nearest-neighbor sites, since the spin background is the same as that of the ground state. Meanwhile, if it involves hopping along y, nonlocal spin strings generically emerge along the DH trajectory. In this case, the pair cannot contribute to $\langle\Psi_{\mathrm{GS}}|\hat{J}_x|\delta\Psi_{\mathrm{ex}}(t)\rangle$ (no recombination), because $\hat{J}_x|\Psi_{\mathrm{GS}}\rangle$ cannot have the same spin configuration as $|\delta\Psi_{\mathrm{ex}}(t)\rangle$ due to the spin strings. This explains the reduction of the subcycle signal for DH pairs with long time intervals and accounts for the decoherence at nonzero t_y. Importantly, this process is active even for $J_{\mathrm{ex}} = 0$, i.e., without energetic coupling between spin and charge. This dephasing mechanism is also confirmed by the dependence of the coherence on the spin polarization, and is absent in conventional semiconductors, see SM.

Next, we discuss the effects of emergent elementary excitations on HHG. To obtain hints on relevant elementary excitations for $t_y = 1$, 2, we analyze the single-particle spectra $A(k_x, k_y, \omega)$ in momentum space, which captures the states accessible by removing (adding) an electron from (to) the system [98]. In Fig. 4, we show $A(k_x, k_y, \omega)$ for

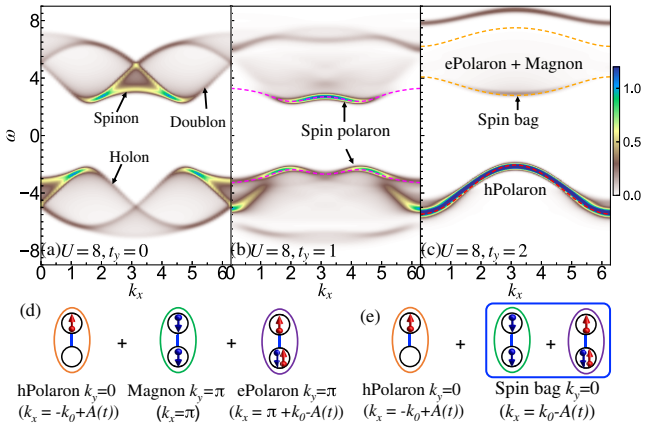

FIG. 4. (a)–(c) Single-particle spectra $A(k_x, k_y = 0, \omega)$ of the half-filled two-leg Hubbard model calculated with DMRG. We set $t_x = 1$ and $U = 8$ and the number of sites along x is 80. Dashed lines in (b) show the dispersion of spin polarons extracted from $A(k_x, k_y = 0, \omega)$. Dashed lines in (c) indicate the dispersion of the hPolaron and the range of the continuum consisting of an ePolaron and a magnon, as predicted by the strong-rung perturbation theory. (d),(e) Two different scenarios of the HHG process in the strong-rung regime.

$k_y = 0$, obtained with the time-dependent density-matrix renormalization group (DMRG) [99,100]. In the present system, k_y is either 0 or π, and $A(k_x, k_y, \omega) = A(k_x + \pi, k_y + \pi, -\omega)$. For $t_y = 0$, dispersive signals corresponding to doublons, holons, and spinons are observed [101,102]. For $t_y = 1$, a low-lying dispersive band ($2.5 \lesssim |\omega| \lesssim 3.5$) corresponding to the formation of spin polarons (charges dressed by spin clouds) emerges [98]. For $t_y = 2$, we see a coherent band for $\omega < 0$ and a continuum around $2.5 \lesssim \omega \lesssim 7.5$. For $t_y = 2$, perturbation theory in the limit of strong-rung coupling works well, see SM. The band for $\omega < 0$ corresponds to a polaron with a positive charge $-q$ (hPolaron) and $k_y = 0$. Meanwhile, the continuum consists of a polaron with a negative charge q (ePolaron) with $k_y = \pi$ and a magnon with $k_y = \pi$. The signal at the bottom of the continuum has high intensity. This signal represents a weakly bound state of an ePolaron and a magnon, a composite particle called a spin bag [98].

We now reveal the role of these elementary excitations. For $t_y = 1$, the first HHG plateau just above the gap aligns with the range of recombination energies of a spin-polaron pair ($4.5 \lesssim \omega \lesssim 6.5$), estimated from their bands in Fig. 4(b). Furthermore, the corresponding subcycle signals are well explained by the three-step model combined with the spin-polaron dispersions, see colored crosses in Fig. 2(c). Thus, the additional plateau can be attributed to the coherent dynamics and recombination of a spin-polaron pair, which explains the nonmonotonic intensity evolution in this regime, see SM. Importantly, at $t_y = 1$, charge dynamics is fractionalized into DH and spin-polaron dynamics due to correlation effects, and HHG captures this physics as two plateaus.

For $t_y = 2$, the following two scenarios based on the three-step picture are conceivable. Since we excite the system with a homogeneous field, the total momentum of the relevant elementary excitations must remain zero. Scenario 1 involves three elementary excitations, a hPolaron with $k_y = 0$, an ePolaron with $k_y = \pi$, and a magnon $k_y = \pi$, see Fig. 4(d). This situation is very different from the conventional scenario, which involves two elementary excitations [103]. Since a magnon carries no charge, only the polarons move around under the electric field to acquire kinetic energy. Still, the magnon balances the total momentum in the tunneling and recombination processes, and yields an energy shift corresponding to its creation energy. Scenario 2 involves two elementary excitations, i.e., one hPolaron and one spin bag, see Fig. 4(e). In Fig. 2(d), we compare the subcycle spectrum and the prediction from the semiclassical theory for the two scenarios. The analysis shows that scenario 1 provides a better explanation of the subcycle signal, which is further confirmed for broad parameter sets, see SM. Scenario 1 consistently explains that the recovery of the coherence of the signal originates from the emergence of coherent

polarons in the strong-rung regime. Still, we note that in $A(k_x, k_y, \omega)$, the $\omega > 0$ part looks incoherent and information on the ePolaron is hidden [Fig. 4(c)]. This result shows that the relation between HHG and the single-particle spectrum is not straightforward, in contrast to semiconductors [44].

Discussion—Our study of the two-leg Hubbard model revealed that the effects of spin-charge couplings on HHG are multifaceted. Experimentally, these characteristic HHG features could be systematically studied in two-leg systems [68,72,104] such as $SrCu_2O_3$ by tuning the ratio t_y/t_x through chemical and physical pressure [77]. Larger modifications of the hopping parameters can be achieved with nonlinear phononics [105]. Information on the subcycle dynamics may be extracted using ultrafast techniques like the time-domain observation of electric fields [106–108], attosecond transient-absorption spectroscopy [109,110], and multidimensional spectroscopy [111].

The many-body effects discussed here should not be limited to two-leg systems. Spin strings and spin polarons also exist in two-dimensional systems [70,71,112], and their effects on HHG should be highly relevant there. We also expect that HHG involving multiple elementary excitations is common in correlated systems. Our results serve as an essential step toward a microscopic understanding of nontrivial HHG features, as reported in various strongly correlated materials [55,58].

The iTEBD calculations have been implemented using the open-source library ITensor [113].

Acknowledgments—We thank T. Ikeda, K. Sugimoto, T. Kaneko, and K. Shinjo for fruitful discussions. This work was supported by Grant-in-Aid for Scientific Research from JSPS, KAKENHI Grants No. JP21H05017 (Y. M.), No. JP24H00191 (Y. M and S. T), No. JP23K22418 (S. T.), No. JP24K06891 (S. T.), JST CREST Grant No. JPMJCR1901 (Y. M.), the RIKEN TRIP initiative RIKEN Quantum (Y. M.), the independent Research Fund Denmark Grant No. 1026-00040B (T. H., L. B. M.), and SNSF Grant No. 200021-196966 (P. W.).

[1] P. B. Corkum and F. Krausz, Nat. Phys. **3**, 381 (2007).
[2] F. Krausz and M. Ivanov, Rev. Mod. Phys. **81**, 163 (2009).
[3] F. Krausz and M. I. Stockman, Nat. Photonics **8**, 205 (2014).
[4] C. Heide, Y. Kobayashi, S. R. U. Haque, and S. Ghimire, Nat. Phys. **20**, 1546 (2024).
[5] M. Ferray, A. L'Huillier, X. F. Li, L. A. Lompre, G. Mainfray, and C. Manus, J. Phys. B **21**, L31 (1988).
[6] P. B. Corkum, Phys. Rev. Lett. **71**, 1994 (1993).
[7] M. Lewenstein, P. Balcou, M. Y. Ivanov, A. L'Huillier, and P. B. Corkum, Phys. Rev. A **49**, 2117 (1994).
[8] S. Ghimire, A. D. DiChiara, E. Sistrunk, P. Agostini, L. F. DiMauro, and D. A. Reis, Nat. Phys. **7**, 138 (2011).
[9] S. Y. Kruchinin, F. Krausz, and V. S. Yakovlev, Rev. Mod. Phys. **90**, 021002 (2018).
[10] S. Ghimire and D. A. Reis, Nat. Phys. **15**, 10 (2019).
[11] E. Goulielmakis and T. Brabec, Nat. Photonics **16**, 411 (2022).
[12] M. Borsch, M. Meierhofer, R. Huber, and M. Kira, Nat. Rev. Mater. **8**, 668 (2023).
[13] O. Schubert, M. Hohenleutner, F. Langer, B. Urbanek, C. Lange, U. Huttner, D. Golde, T. Meier, M. Kira, S. W. Koch, and R. Huber, Nat. Photonics **8**, 119 (2014).
[14] G. Vampa, C. R. McDonald, G. Orlando, D. D. Klug, P. B. Corkum, and T. Brabec, Phys. Rev. Lett. **113**, 073901 (2014).
[15] T. T. Luu, M. Garg, S. Y. Kruchinin, A. Moulet, M. T. Hassan, and E. Goulielmakis, Nature (London) **521**, 498 (2015).
[16] G. Vampa, T. J. Hammond, N. Thire, B. E. Schmidt, F. Legare, C. R. McDonald, T. Brabec, and P. B. Corkum, Nature (London) **522**, 462 (2015).
[17] F. Langer, M. Hohenleutner, C. P. Schmid, C. Pöllmann, P. Nagler, T. Korn, C. Schüller, M. Sherwin, U. Huttner, J. Steiner, S. Koch, M. Kira, and R. Huber, Nature (London) **533**, 225 (2016).
[18] M. Hohenleutner, F. Langer, O. Schubert, M. Knorr, U. Huttner, S. Koch, M. Kira, and R. Huber, Nature (London) **523**, 572 (2015).
[19] G. Ndabashimiye, S. Ghimire, M. Wu, D. A. Browne, K. J. Schafer, M. B. Gaarde, and D. A. Reis, Nature (London) **534**, 520 (2016).
[20] T. Otobe, Phys. Rev. B **94**, 235152 (2016).
[21] N. Tancogne-Dejean, O. D. Mücke, F. X. Kärtner, and A. Rubio, Nat. Commun. **8**, 745 (2017).
[22] T. Ikemachi, Y. Shinohara, T. Sato, J. Yumoto, M. Kuwata-Gonokami, and K. L. Ishikawa, Phys. Rev. A **95**, 043416 (2017).
[23] H. Liu, Y. Li, Y. S. You, S. Ghimire, T. F. Heinz, and D. A. Reis, Nat. Phys. **13**, 262 (2017).
[24] Y. S. You, D. Reis, and S. Ghimire, Nat. Phys. **13**, 345 (2017).
[25] K. Kaneshima, Y. Shinohara, K. Takeuchi, N. Ishii, K. Imasaka, T. Kaji, S. Ashihara, K. L. Ishikawa, and J. Itatani, Phys. Rev. Lett. **120**, 243903 (2018).
[26] F. Sekiguchi, G. Yumoto, H. Hirori, and Y. Kanemitsu, Phys. Rev. B **106**, L241201 (2022).
[27] F. Giorgianni *et al.*, Nat. Commun. **7**, 11421 (2016).
[28] N. Yoshikawa, T. Tamaya, and K. Tanaka, Science **356**, 736 (2017).
[29] H. A. Hafez, S. Kovalev, J.-C. Deinert, Z. Mics, B. Green, N. Awari, M. Chen, S. Germanskiy, U. Lehnert, J. Teichert, Z. Wang, K.-J. Tielrooij, Z. Liu, Z. Chen, A. Narita, K. Mullen, M. Bonn, M. Gensch, and D. Turchinovich, Nature (London) **561**, 507 (2018).
[30] R. E. F. Silva, Á. Jiménez-Galán, B. Amorim, O. Smirnova, and M. Ivanov, Nat. Photonics **13**, 849 (2019).
[31] A. Chacón, D. Kim, W. Zhu, S. P. Kelly, A. Dauphin, E. Pisanty, A. S. Maxwell, A. Picón, M. F. Ciappina, D. E. Kim, C. Ticknor, A. Saxena, and M. Lewenstein, Phys. Rev. B **102**, 134115 (2020).
[32] B. Cheng, N. Kanda, T. N. Ikeda, T. Matsuda, P. Xia, T. Schumann, S. Stemmer, J. Itatani, N. P. Armitage, and R. Matsunaga, Phys. Rev. Lett. **124**, 117402 (2020).

[33] C. P. Schmid, L. Weigl, P. Grössing, V. Junk, C. Gorini, S. Schlauderer, S. Ito, M. Meierhofer, N. Hofmann, D. Afanasiev, J. Crewse, K. A. Kokh, O. E. Tereshchenko, J. Güdde, F. Evers, J. Wilhelm, K. Richter, U. Höfer, and R. Huber, Nature (London) **593**, 385 (2021).

[34] D. Baykusheva, A. Chacón, J. Lu, T. P. Bailey, J. A. Sobota, H. Soifer, P. S. Kirchmann, C. Rotundu, C. Uher, T. F. Heinz, D. A. Reis, and S. Ghimire, Nano Lett. **21**, 8970 (2021).

[35] R. E. F. Silva, I. V. Blinov, A. N. Rubtsov, O. Smirnova, and M. Ivanov, Nat. Photonics **12**, 266 (2018).

[36] Y. Murakami, M. Eckstein, and P. Werner, Phys. Rev. Lett. **121**, 057405 (2018).

[37] N. Tancogne-Dejean, M. A. Sentef, and A. Rubio, Phys. Rev. Lett. **121**, 097402 (2018).

[38] J. Freudenstein, M. Borsch, M. Meierhofer, D. Afanasiev, C. P. Schmid, F. Sandner, M. Liebich, A. Girnghuber, M. Knorr, M. Kira, and R. Huber, Nature (London) **610**, 290 (2022).

[39] S. Imai, A. Ono, and S. Ishihara, Phys. Rev. Lett. **124**, 157404 (2020).

[40] S. Takayoshi, Y. Murakami, and P. Werner, Phys. Rev. B **99**, 184303 (2019).

[41] T. N. Ikeda and M. Sato, Phys. Rev. B **100**, 214424 (2019).

[42] A. Roy, S. Bera, and K. Saha, Phys. Rev. Res. **2**, 043133 (2020).

[43] G. McCaul, C. Orthodoxou, K. Jacobs, G. H. Booth, and D. I. Bondar, Phys. Rev. Lett. **124**, 183201 (2020).

[44] Y. Murakami, S. Takayoshi, A. Koga, and P. Werner, Phys. Rev. B **103**, 035110 (2021).

[45] C. Orthodoxou, A. Zaïr, and G. H. Booth, npj Quantum Mater. **6**, 76 (2021).

[46] M. Udono, K. Sugimoto, T. Kaneko, and Y. Ohta, Phys. Rev. B **105**, L241108 (2022).

[47] M. R. Bionta, E. Haddad, A. Leblanc, V. Gruson, P. Lassonde, H. Ibrahim, J. Chaillou, N. Émond, M. R. Otto, A. Jiménez-Galán, R. E. F. Silva, M. Ivanov, B. J. Siwick, M. Chaker, and F. Légaré, Phys. Rev. Res. **3**, 023250 (2021).

[48] W. Zhu, B. Fauseweh, A. Chacon, and J.-X. Zhu, Phys. Rev. B **103**, 224305 (2021).

[49] C. Shao, H. Lu, X. Zhang, C. Yu, T. Tohyama, and R. Lu, Phys. Rev. Lett. **128**, 047401 (2022).

[50] T. Hansen, Simon Vendelbo Bylling Jensen, and L. B. Madsen, Phys. Rev. A **105**, 053118 (2022).

[51] K. Uchida, G. Mattoni, S. Yonezawa, F. Nakamura, Y. Maeno, and K. Tanaka, Phys. Rev. Lett. **128**, 127401 (2022).

[52] Y. Murakami, K. Uchida, A. Koga, K. Tanaka, and P. Werner, Phys. Rev. Lett. **129**, 157401 (2022).

[53] T. Hansen and L. B. Madsen, Phys. Rev. B **106**, 235142 (2022).

[54] O. Gränäs *et al.*, Phys. Rev. Res. **4**, L032030 (2022).

[55] J. Alcalà, U. Bhattacharya, J. Biegert, M. Ciappina, U. Elu, T. Graß, P. T. Grochowski, M. Lewenstein, A. Palau, T. P. H. Sidiropoulos, T. Steinle, and I. Tyulnev, Proc. Natl. Acad. Sci. U.S.A. **119**, e2207766119 (2022).

[56] J. Masur, D. I. Bondar, and G. McCaul, Phys. Rev. A **106**, 013110 (2022).

[57] D. Alam, N. Ud Din, M. Chini, and V. Turkowski, Phys. Rev. B **106**, 235124 (2022).

[58] A. Nakano, K. Uchida, Y. Tomioka, M. Takaya, Y. Okimoto, and K. Tanaka, Phys. Rev. Res. **6**, L042032 (2024).

[59] A. AlShafey, G. McCaul, Y.-M. Lu, X.-Y. Jia, S.-S. Gong, Z. Addison, D. I. Bondar, M. Randeria, and A. S. Landsman, Phys. Rev. B **108**, 144434 (2023).

[60] K. Huang and T.-Y. Du, Phys. Rev. B **108**, 155125 (2023).

[61] A. Ono, S. Okumura, S. Imai, and Y. Akagi, Phys. Rev. B **110**, 125111 (2024).

[62] N. M. Allafi, M. H. Kolodrubetz, M. Bukov, V. Oganesyan, and M. Yarmohammadi, Phys. Rev. B **110**, 064420 (2024).

[63] F. Queisser and R. Schützhold, Phys. Rev. B **109**, 205110 (2024).

[64] S. Pooyan and D. Bauer, arXiv:2406.04114.

[65] G. L. Prajapati, S. Ray, I. Ilyakov, A. N. Ponomaryov, A. Arshad, T. V. A. G. de Oliveira, G. Dubey, D. S. Rana, J.-C. Deinert, P. Werner, and S. Kovalev, arXiv:2410.01424.

[66] M. Dziurawiec, J. O. de Almeida, M. L. Bera, M. Plodzien, M. Lewenstein, T. Grass, R. W. Chhajlany, M. M. Maska, and U. Bhattacharya, arXiv:2404.14411.

[67] E. Dagotto, Rev. Mod. Phys. **66**, 763 (1994).

[68] M. Imada, A. Fujimori, and Y. Tokura, Rev. Mod. Phys. **70**, 1039 (1998).

[69] Y. Murakami, D. Golež, M. Eckstein, and P. Werner, arXiv:2310.05201.

[70] G. Ji, M. Xu, L. H. Kendrick, C. S. Chiu, J. C. Brüggenjürgen, D. Greif, A. Bohrdt, F. Grusdt, E. Demler, M. Lebrat, and M. Greiner, Phys. Rev. X **11**, 021022 (2021).

[71] A. Bohrdt, E. Demler, F. Pollmann, M. Knap, and F. Grusdt, Phys. Rev. B **102**, 035139 (2020).

[72] E. Dagotto and T. M. Rice, Science **271**, 618 (1996).

[73] R. M. Noack, S. R. White, and D. J. Scalapino, Phys. Rev. Lett. **73**, 882 (1994).

[74] L. Balents and M. P. A. Fisher, Phys. Rev. B **53**, 12133 (1996).

[75] R. Noack, S. White, and D. Scalapino, Physica (Amsterdam) **270C**, 281 (1996).

[76] T. F. A. Müller, V. Anisimov, T. M. Rice, I. Dasgupta, and T. Saha-Dasgupta, Phys. Rev. B **57**, R12655 (1998).

[77] H. Sakamoto and K. Kuroki, Phys. Rev. Res. **2**, 022055(R) (2020).

[78] G. Vidal, Phys. Rev. Lett. **98**, 070201 (2007).

[79] See Supplemental Material at http://link.aps.org/supplemental/10.1103/PhysRevLett.134.096504 for details of the formulation and additional results, which includes Refs. [80–93].

[80] E. M. Stoudenmire and S. R. White, New J. Phys. **12**, 055026 (2010).

[81] J. Ostmeyer, J. Phys. A **56**, 285303 (2023).

[82] T. Barthel and Y. Zhang, Ann. Phys. (Amsterdam) **418**, 168165 (2020).

[83] A. Alvermann and H. Fehske, J. Comput. Phys. **230**, 5930 (2011).

[84] J. Haegeman, C. Lubich, I. Oseledets, B. Vandereycken, and F. Verstraete, Phys. Rev. B **94**, 165116 (2016).

[85] C. N. Yang, Phys. Rev. Lett. **63**, 2144 (1989).

[86] H. Endres, R. M. Noack, W. Hanke, D. Poilblanc, and D. J. Scalapino, Phys. Rev. B **53**, 5530 (1996).
[87] A. L. Fetter and J. D. Walecka, *Quantum Theory of Many-Particle Systems* (Dover Publications, New York, 2003).
[88] J. A. Sobota, Y. He, and Z.-X. Shen, Rev. Mod. Phys. **93**, 025006 (2021).
[89] K. Shinjo, Y. Tamaki, S. Sota, and T. Tohyama, Phys. Rev. B **104**, 205123 (2021).
[90] N. Yoshikawa, K. Nagai, K. Uchida, Y. Takaguchi, S. Sasaki, Y. Miyata, and K. Tanaka, Nat. Commun. **10**, 1 (2019).
[91] J. Li, D. Golez, G. Mazza, A. J. Millis, A. Georges, and M. Eckstein, Phys. Rev. B **101**, 205140 (2020).
[92] M. Schüler, J. A. Marks, Y. Murakami, C. Jia, and T. P. Devereaux, Phys. Rev. B **103**, 155409 (2021).
[93] S. Imai, A. Ono, and S. Ishihara, Phys. Rev. Res. **4**, 043155 (2022).
[94] O. Neufeld, D. Podolsky, and O. Cohen, Nat. Commun. **10**, 405 (2019).
[95] C. S. Lange, T. Hansen, and L. B. Madsen, Phys. Rev. A **109**, 063103 (2024).
[96] A. H. MacDonald, S. M. Girvin, and D. Yoshioka, Phys. Rev. B **37**, 9753 (1988).
[97] Y. Murakami, S. Takayoshi, T. Kaneko, Z. Sun, D. Golež, A. J. Millis, and P. Werner, Commun. Phys. **5**, 23 (2022).
[98] C. Yang and A. E. Feiguin, Phys. Rev. B **99**, 235117 (2019).
[99] S. R. White and A. E. Feiguin, Phys. Rev. Lett. **93**, 076401 (2004).
[100] J. Haegeman, J. I. Cirac, T. J. Osborne, I. Pižorn, H. Verschelde, and F. Verstraete, Phys. Rev. Lett. **107**, 070601 (2011).
[101] F. H. L. Essler, H. Frahm, F. Göhmann, A. Klümper, and V. E. Korepin, *The One-Dimensional Hubbard Model* (Cambridge University Press, Cambridge, England, 2005).
[102] A. Bohrdt, D. Greif, E. Demler, M. Knap, and F. Grusdt, Phys. Rev. B **97**, 125117 (2018).
[103] G. Vampa, C. R. McDonald, G. Orlando, P. B. Corkum, and T. Brabec, Phys. Rev. B **91**, 064302 (2015).
[104] P. Abbamonte, G. Blumberg, A. Rusydi, A. Gozar, P. G. Evans, T. Siegrist, L. Venema, H. Eisaki, E. D. Isaacs, and G. A. Sawatzky, Nature (London) **431**, 1078 (2004).
[105] M. Först, C. Manzoni, S. Kaiser, Y. Tomioka, Y. Tokura, R. Merlin, and A. Cavalleri, Nat. Phys. **7**, 854 (2011).
[106] S. B. Park, K. Kim, W. Cho, S. I. Hwang, I. Ivanov, C. H. Nam, and K. T. Kim, Optica **5**, 402 (2018).
[107] W. Cho, S. I. Hwang, C. H. Nam, M. R. Bionta, P. Lassonde, B. E. Schmidt, H. Ibrahim, F. Légaré, and K. T. Kim, Sci. Rep. **9**, 16067 (2019).
[108] P. D. Keathley, S. V. B. Jensen, M. Yeung, M. R. Bionta, and L. B. Madsen, Phys. Rev. B **107**, 054302 (2023).
[109] M. Wu, S. Chen, S. Camp, K. J. Schafer, and M. B. Gaarde, J. Phys. B **49**, 062003 (2016).
[110] J. E. Bækhøj, L. Yue, and L. B. Madsen, Phys. Rev. A **91**, 043408 (2015).
[111] V. N. Valmispild, E. Gorelov, M. Eckstein, A. I. Lichtenstein, H. Aoki, M. I. Katsnelson, M. Y. Ivanov, and O. Smirnova, Nat. Photonics **18**, 432 (2024).
[112] C. Yang and A. E. Feiguin, Phys. Rev. B **93**, 081107(R) (2016).
[113] M. Fishman, S. R. White, and E. M. Stoudenmire, SciPost Phys. Codebases 4 (2022).